ACS OMEGA

Article

Cite This: ACS Omega 2018, 3, 10033−10041

http://pubs.acs.org/journal/acsodf

Comparative Study on the Supramolecular Assemblies Formed by Calixpyridinium and Two Alginates with Different Viscosities

Kui Wang,* Meng-Meng Wang, Hong-Xi Dou, Si-Yang Xing,* Bo-Lin Zhu,* and Jian-Hua Cui

Tianjin Key Laboratory of Structure and Performance for Functional Molecules, Key Laboratory of Inorganic−Organic Hybrid Functional Materials Chemistry, Ministry of Education, College of Chemistry, Tianjin Normal University, Tianjin 300387, China

Supporting Information

ABSTRACT: In this work, a comparative study on the supramolecular assemblies formed by calixpyridinium and two alginates with different viscosities was performed. We found that sodium alginate (SA) with medium viscosity (SA-M) had a better capability to induce aggregation of calixpyridinium in comparison with SA with low viscosity (SA-L) because of the stronger electrostatic interactions between calixpyridinium and SA-M. Therefore, the morphology of calixpyridinium−SA-M supramolecular aggregates was a compact spherical structure, while that of calixpyridinium−SA-L supramolecular aggregates was an incompact lamellar structure. As a result, adding much more amount of 1,3,6,8-pyrenetetrasulfonic acid tetrasodium salt to calixpyridinium−SA-M solution was required to achieve the balance of the competitive binding, and in comparison with calixpyridinium−SA-L supramolecular aggregates, calixpyridinium−SA-M supramolecular aggregates were more sensitive to alkali. However, for the same reason, in comparison with calixpyridinium−SA-M supramolecular aggregates, calixpyridinium−SA-L supramolecular aggregates were much more stable in water not only at room temperature but also at a higher temperature, and even in salt solution. Therefore, in comparison with calixpyridinium−SA-L supramolecular aggregates, calixpyridinium−SA-M supramolecular aggregates exhibited a completely opposite response to acid because of the generation of salt. Because SA is an important biomaterial with excellent biocompatibility, it is anticipated that this comparative study is extremely important in constructing functional supramolecular biomaterials.

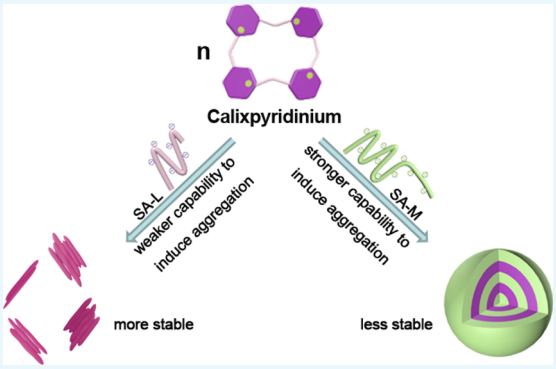

1. INTRODUCTION

Self-assembly phenomena are ubiquitous in many fields, such as materials science, chemistry, and biology.[1] Nature has provided many cases that well elucidate this concept, for example, membrane structures in the endoplasmic reticulum and stem cells.[2] The assembled structures can be precisely controlled by the ingenious design of the building units.[3] In this context, the construction of well-defined nanoscaled or microscaled structures based on molecular self-assembly remains a key challenge facing modern chemistry. So far, many noncovalent interactions, such as $\pi\cdots\pi$, charge-transfer, and hydrogen-bonding interactions, among others,[4] have been widely applied in fabricating different kinds of structured aggregates via molecular self-assembly, including fibers, vesicles, tubules, disks, and micelles.[5] However, these commonly used intermolecular interactions are not always effective in pure water. As a result, most of these assemblies lack the necessary biocompatibility for applications in biological, medical, and environmental arenas. The host−guest interactions based on macrocycles, for example, *p*-sulfonatocalixarenes, modified-pillararenes, cyclodextrins, and cucurbiturils, occur usually in water.[6] Consequently, the host−guest interactions based on macrocyclic receptors are particularly advantageous in fabricating water-soluble assemblies.[7] It is noted that most of these frequently used macrocyclic receptors are perfect hosts for cationic guests. The construction of water-soluble assemblies through the anionic recognition of macrocyclic receptors has been explored much less frequently because the recognition of anions in water remains a key challenge in modern supramolecular chemistry.[8] In fact, anionic species are very important because of their biological and environmental relevance.[9]

Positively charged calixpyridinium, obtained by the intermolecular cyclization of 3-bromomethylpyridine,[10] is water-soluble. Moreover, this cationic macrocyclic receptor has exhibited good inclusion/complexation properties for anionic guests. Shinoda et al. first studied the host−guest interactions between calixpyridinium and tricarboxylate anions in 1998, and they found that the geometry of the three carboxyl groups in guests is the key factor for determining the affinity and selectivity of host−guest complexation.[10] Atilgan and Akkaya provided the first case of applying macrocyclic calixpyridinium in fluorescence sensing of anions by the indicator displacement method in 2004, and they found that the affinities of

Received: July 6, 2018
Accepted: July 31, 2018
Published: August 28, 2018

DOI: 10.1021/acsomega.8b01554
ACS Omega 2018, 3, 10033−10041

calixpyridinium for anionic guests were determined by the total negative charges of anionic species.[9a] In 2016, we fabricated a novel reporter pair based on calixpyridinium in supramolecular tandem assay for continuous and real-time monitoring of alkaline phosphatase activity by taking advantage of the selective binding of calixpyridinium toward anionic adenosine triphosphate and its hydrolysis products catalyzed by alkaline phosphatase.[11] In 2017, we found the highly selective binding of calixpyridinium toward acidic amino acids in aqueous media, and the electrostatic interactions between positively charged calixpyridinium and anionic acidic amino acids are the main driving forces.[12] Although calixpyridinium has exhibited good binding ability to anionic guests, the construction of water-soluble supramolecular assemblies via the anionic recognition of calixpyridinium has been explored much less frequently. Last year, we fabricated the first supramolecular assembly based on the anionic recognition of calixpyridinium, in which native biocompatible polysaccharide hyaluronan was employed as the guest.[13] Recently, we successfully constructed another calixpyridinium-based supramolecular assembly employing polyanionic chondroitin 4-sulfate as the guest.[14] Compared with calixpyridinium−hyaluronan assembly, the stability of calixpyridinium−chondroitin 4-sulfate assembly is better because of the stronger electrostatic interactions between the host and the guest originating from the higher negative charge density on the side chain of chondroitin 4-sulfate.

Alginic acid, produced by some bacteria and brown algae, such as *Azotobacter*- and *Pseudomonas* species,[15] is a naturally occurring linear polyuronic acid. Sodium alginate (SA), the sodium salt of alginic acid, has attracted more and more attention of researchers[16] because it is a very important biomaterial with good biocompatibility. However, up to now, supramolecular material constructed via the host−guest interactions of macrocyclic receptors with SA has been explored much less frequently. Herein, we report a comparative study on the supramolecular assemblies formed by calixpyridinium and two alginates with different viscosities (Scheme 1), SA with low viscosity (SA-L) and SA with medium viscosity (SA-M). It is anticipated that this comparative study is extremely important, not only in further understanding the assembling mechanism of the calixpyridinium receptor with polyanion, but also in constructing functional supramolecular biomaterials.

2. RESULTS AND DISCUSSION

The optical transmittance of different concentrations of SA solution was first detected to measure the critical aggregation concentration (CAC) of polysaccharide SA because pure SA may self-aggregate in water (Figure S1). As shown in Figure S1a, increasing the concentration of SA-L from 0.05 to 0.20 mg/mL could not lead to any change in its optical transmittance over 350 nm. With the addition of more SA-L (from 0.20 to 2.01 mg/mL), its optical transmittance over 350 nm began to decrease gradually because of the turbidity generated by the aggregation of SA-L. The CAC value of pure SA-L (0.74 mg/mL) could therefore be measured by observing the inflection point on the plot of the optical transmittance at 350 nm of SA-L versus their concentrations (Figure 1a). A similar experimental phenomenon was observed for SA-M (Figure S1b), and the obtained CAC value of pure SA-M (0.68 mg/mL) was also quite similar to that of pure SA-L (Figure 1b), suggesting that free SA with different viscosities has similar aggregation ability.

Scheme 1. Schematic Illustration of the Comparative Study on the Supramolecular Assemblies Formed by Calixpyridinium and Two Alginates with Different Viscosities

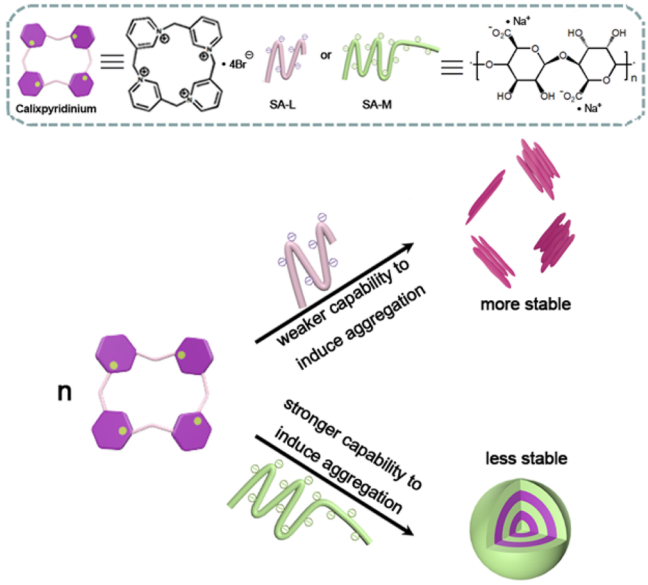

Next, we added calixpyridinium gradually to a solution of SA-L at a fixed concentration that is far lower than its CAC, and we found that the addition of a small quantity of calixpyridinium could not lead to any change in its optical transmittance over 350 nm. With the addition of more calixpyridinium, its optical transmittance over 350 nm began to decrease sharply because of the turbidity generated by polyanionic SA-L-complexation-induced aggregation of cationic calixpyridinium (Figure S2). The SA-L-complexation-induced CAC value of calixpyridinium could therefore be measured by observing the inflection point on the plot of the optical transmittance at 350 nm of calixpyridinium versus their concentrations (Figure 2): 13.4 μM at 13 μg/mL SA-L, 22.5 μM at 24 μg/mL SA-L, 39.2 μM at 50 μg/mL SA-L, 52.1 μM at 70 μg/mL SA-L, 56.3 μM at 96 μg/mL SA-L, and 63.5 μM at 120 μg/mL SA-L. Moreover, we found that SA-L complexation-induced CAC values of calixpyridinium increased linearly with SA-L concentrations in a certain concentration range (Figure 3). Similar experimental phenomena were observed for SA-M (Figures S3 and S4), but the CAC values of calixpyridinium induced by the complexation of SA-M were a little lower than those induced by the complexation of SA-L: 12.6 μM at 13 μg/mL SA-M, 17.0 μM at 24 μg/mL SA-M, 27.9 μM at 50 μg/mL SA-M, 41.4 μM at 70 μg/mL SA-M, 47.4 μM at 96 μg/mL SA-M, and 47.6 μM at 120 μg/mL SA-M, implying that SA-M had a better capability to induce aggregation of calixpyridinium. It is noted that free calixpyridinium cannot self-aggregate in water (Figure S5).

Because different concentrations of SA can all induce aggregation of calixpyridinium, it is necessary to study the best mixing ratio of calixpyridinium and SA for forming calixpyridinium−SA binary supramolecular aggregates. We added SA-L gradually to a solution of calixpyridinium at a fixed concentration of 55 μM. We found that the addition of SA-L first led to a sharp decrease of its optical transmittance over 350 nm because of the turbidity generated by polyanionic SA-L-complexation-induced aggregation of cationic calixpyr-

DOI: 10.1021/acsomega.8b01554
ACS Omega 2018, 3, 10033−10041

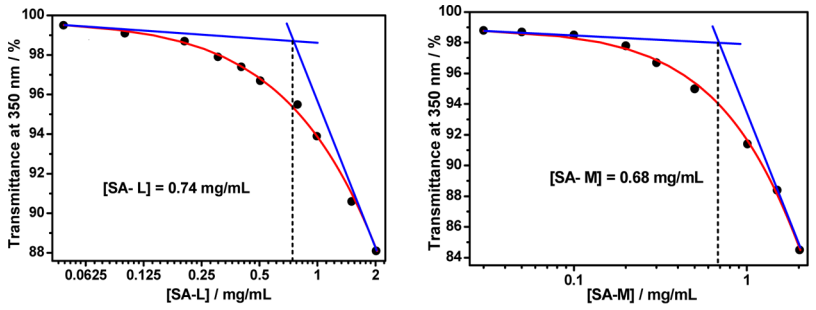

Figure 1. Dependence of the optical transmittance (at 350 nm) of (a) SA-L and (b) SA-M in water vs their concentrations.

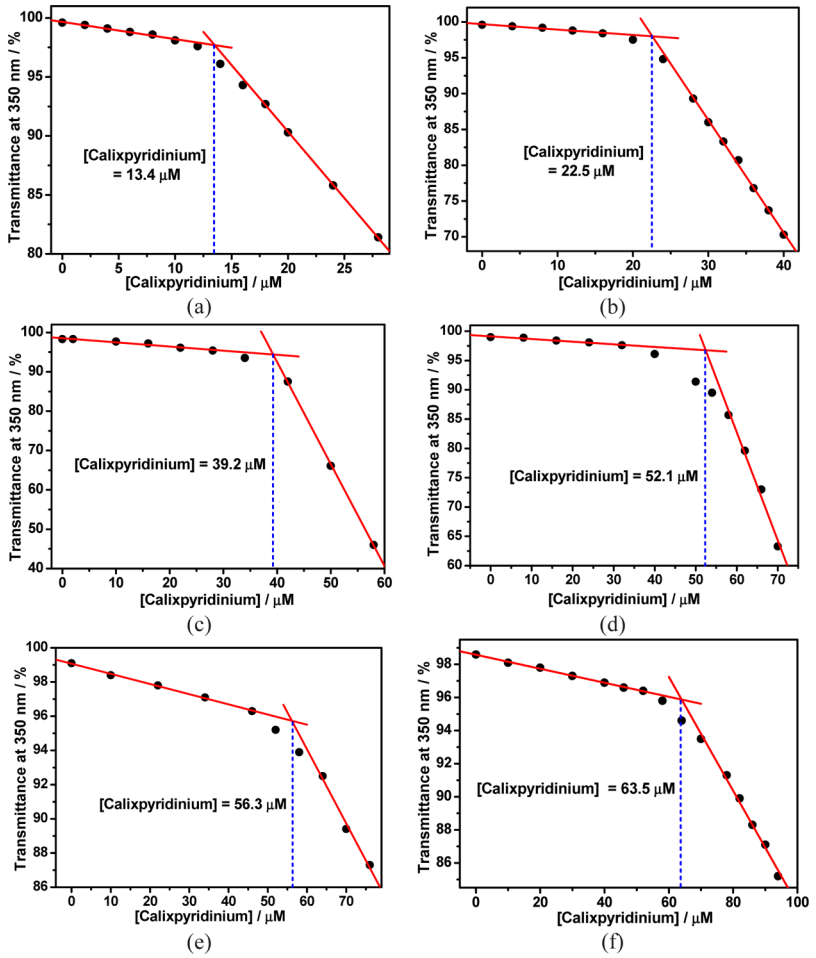

Figure 2. Dependence of the optical transmittance (at 350 nm) of calixpyridinium in water vs their concentrations in the presence of 13 (a), 24 (b), 50 (c), 70 (d), 96 (e), and 120 μg/mL (f) SA-L.

idinium, and with the addition of excess SA-L, its optical transmittance over 350 nm began to increase gradually because of the disassembly of the aggregates, which is more favorable for the entropy term (Figure S6a). The best concentration of SA-L (50 μg/mL) for the formation of calixpyridinium−SA-L supramolecular aggregates could therefore be measured by observing the inflection point on the plot of the optical transmittance at 350 nm of SA-L versus their concentrations (Figure 4a). A similar experimental phenomenon was observed for SA-M (Figure S6b), but the obtained best concentration of SA-M (40 μg/mL) is a little lower than that of SA-L for the formation of calixpyridinium−SA-M supramolecular aggregates when the concentration of calixpyridinium is also fixed at 55 μM (Figure 4b), which again implied that SA-M had a better capability to induce aggregation of calixpyridinium. Further studies on the supramolecular assemblies between calixpyridinium and SA were based on these ratios. It is noted that 1-methylpyridinium (the building subunit of calixpyridinium) and SA cannot form supramolecular aggregates (Figure S7), implying that the cyclic structure of the host is also a key factor for the construction of calixpyridinium−SA supramolecular aggregates.

The stability of calixpyridinium−SA supramolecular aggregates was further studied at room and higher temperatures. As can be seen from Figure 5a, there was no appreciable change in the transmittance spectra of calixpyridinium−SA-L solution

DOI: 10.1021/acsomega.8b01554
ACS Omega 2018, 3, 10033−10041

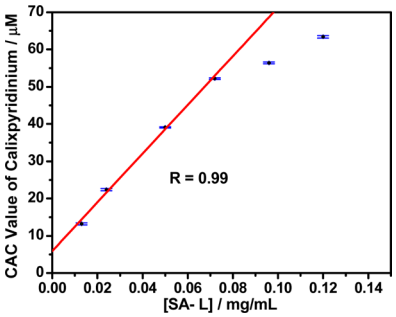

Figure 3. Linear relationship between the CAC values of calixpyridinium and the concentrations of SA-L in water.

over 7 days at room temperature. Moreover, the optical transmittance could not be disturbed either by centrifuging the calixpyridinium−SA-L solution for 1 min at 3000 rpm (Figure 6a), or by increasing the temperature of the calixpyridinium−SA-L solution up to 80 °C (Figure 7a). All of these experimental results indicate that calixpyridinium−SA-L supramolecular aggregates have sufficient stability not only at room temperature but also at a higher temperature. However, as can be seen from Figure 5b, there was an obvious change in the transmittance spectra of calixpyridinium−SA-M solution after only 24 h. Moreover, the optical transmittance was seriously disturbed either by centrifuging the calixpyridinium−SA-M solution (Figure 6b), or by increasing the temperature of the calixpyridinium−SA-M solution (Figure 7b). All of these experimental results reflect that in comparison with calixpyridinium−SA-L supramolecular aggregates, calixpyridinium−SA-M supramolecular aggregates are much less stable not only at room temperature but also at a higher temperature. The surface charge distribution of calixpyridinium−SA supramolecular aggregates was further identified by using zeta potential measurement, giving an average zeta potential of 12.98 for calixpyridinium−SA-L supramolecular aggregates and 10.33 for calixpyridinium−SA-M supramolecular aggregates. The little higher zeta potential of calixpyridinium−SA-L supramolecular aggregates also supported the fact that SA-L could form more stable supramolecular aggregates with calixpyridinium in water.

It is well-known that the stability of the assembly driven by electrostatic interactions would be affected by salt. Therefore, the stability of calixpyridinium−SA supramolecular aggregates in NaCl solution was further studied. As shown in Figure 8a, when the concentration of NaCl was increased from 0 to 15 mM, the optical transmittance of calixpyridinium−SA-L solution was almost unchanged, implying that calixpyridinium−SA-L supramolecular aggregates were even quite stable in NaCl solution. However, as can be seen from Figure 8b, there was an obvious increase in the optical transmittance of calixpyridinium−SA-M solution with the concentration of NaCl increased from 0 to 15 mM as a result of the disassembly of the aggregates, indicating that calixpyridinium−SA-M supramolecular aggregates were more affected by salt in comparison with calixpyridinium−SA-L supramolecular aggregates. One reasonable explanation is that SA-M possesses more negative charges than SA-L, and therefore affords stronger electrostatic interactions with calixpyridinium, which is less stable in water and more affected by salt. The stronger electrostatic interactions between SA-M and calixpyridinium also explain well why SA-M has a better capability to induce aggregation of calixpyridinium.

It has been proved that calixpyridinium and 1,3,6,8-pyrenetetrasulfonic acid tetrasodium salt (PyTS) can form a stable complex in water.[11] On the basis of that, next we would like to explore the disassembly of the calixpyridinium−SA supramolecular aggregates driven by the competitive binding of PyTS with calixpyridinium. As was expected, with the gradual addition of PyTS, there was a gradual increase in the optical transmittance of the calixpyridinium−SA-L solution over 425 nm because of the disassembly of the calixpyridinium−SA-L aggregates (Figure S8a), and as shown in Figure 9a, only ca. 3 equiv of PyTS was needed to achieve the balance of this competitive binding. A similar experimental phenomenon was observed for SA-M (Figure S8b). However, much more amount of PyTS (ca. 32 equiv) was required to achieve the balance of this competitive binding (Figure 9b), although the binding constant between calixpyridinium and PyTS is high up to 10^6 M^{-1},[11] which also implies the stronger electrostatic interactions of SA-M with calixpyridinium.

The responsiveness of calixpyridinium−SA supramolecular aggregates to acid and alkali was further studied because both calixpyridinium and SA could be affected by the pH value. As can be seen from Figure 10a, increasing pH from 6 to 7 could not lead to an obvious change in the optical transmittance of the calixpyridinium−SA-L solution over 700 nm, and further increasing pH to 9 would lead to a dramatic increase in the optical transmittance over 700 nm because of the disassembly of the calixpyridinium−SA-L aggregates, which was also proven by the obvious reduction of the turbidity and Tyndall effect (Figure 11). A reasonable explanation for the disassembly of the calixpyridinium−SA-L aggregates under alkaline condition is that the methylene bridges in calixpyr-

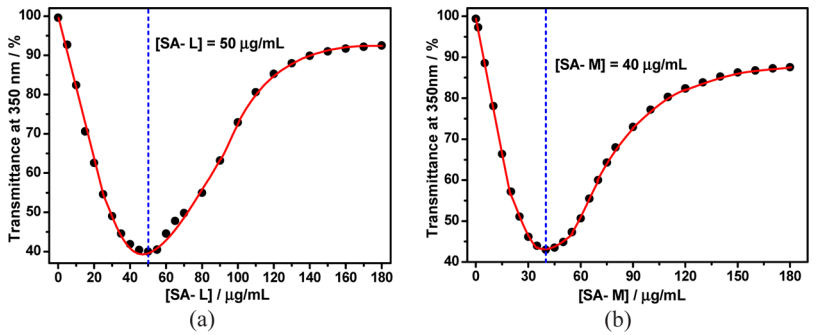

Figure 4. Dependence of the optical transmittance (at 350 nm) of (a) SA-L and (b) SA-M in water vs their concentrations with a fixed calixpyridinium concentration of 55 μM.

DOI: 10.1021/acsomega.8b01554
ACS Omega 2018, 3, 10033−10041

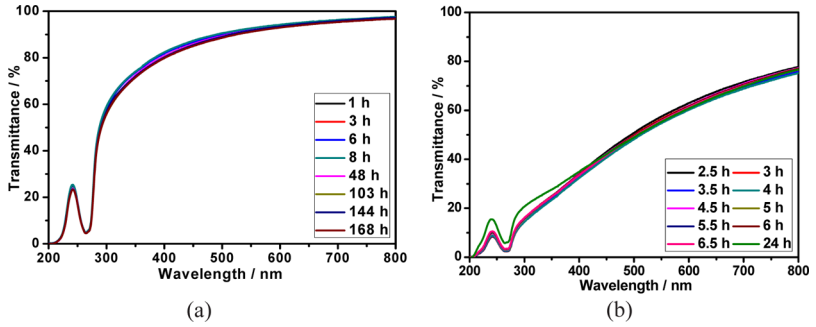

Figure 5. (a) Optical transmittance of the calixpyridinium−SA-L assembly at different times within 7 days at room temperature in water. (b) Optical transmittance of the calixpyridinium−SA-M assembly at different times within 24 h at room temperature in water. [Calixpyridinium] = 55 μM, [SA-L] = 50 μg/mL, and [SA-M] = 40 μg/mL.

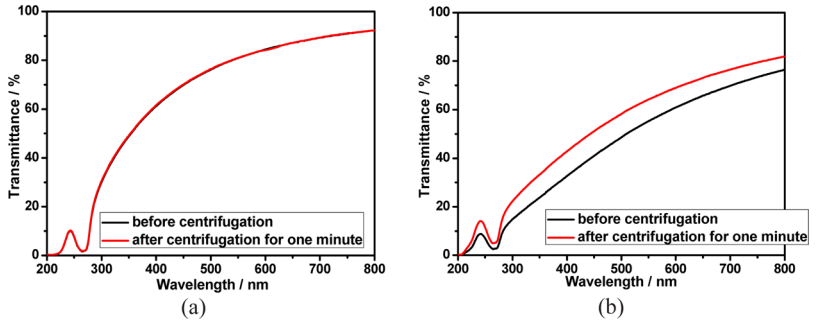

Figure 6. Optical transmittance of calixpyridinium−SA-L (a) and calixpyridinium−SA-M (b) assemblies before and after centrifugation for 1 min at 3000 rpm in aqueous solution. [Calixpyridinium] = 55 μM, [SA-L] = 50 μg/mL, and [SA-M] = 40 μg/mL.

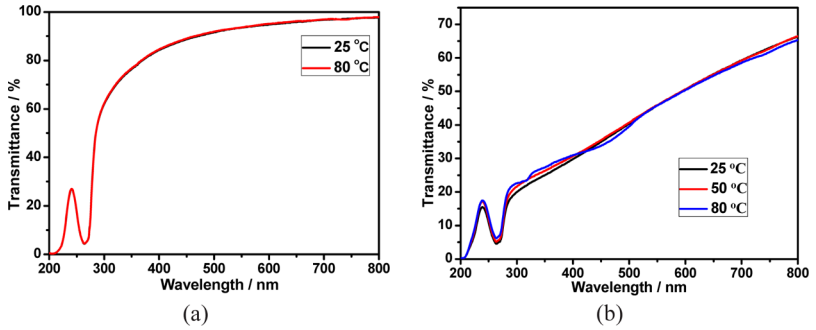

Figure 7. (a) Optical transmittance of the calixpyridinium−SA-L assembly at 25 and 80 °C in water. (b) Optical transmittance of the calixpyridinium−SA-M assembly at 25, 50, and 80 °C in water. [Calixpyridinium] = 55 μM, [SA-L] = 50 μg/mL, and [SA-M] = 40 μg/mL.

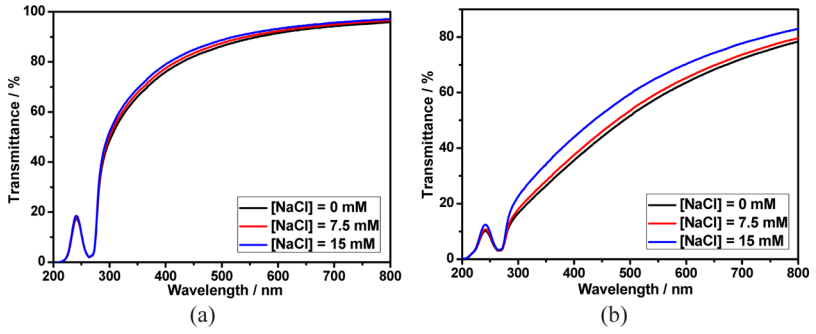

Figure 8. Optical transmittance of calixpyridinium−SA-L (a) and calixpyridinium−SA-M (b) assemblies at different concentrations of NaCl solution. [Calixpyridinium] = 55 μM, [SA-L] = 50 μg/mL, and [SA-M] = 40 μg/mL.

idinium are acidic,[9a] which would be deprotonated under alkaline condition (Figure S9) and therefore result in a weaker electrostatic interaction of calixpyridinium to SA-L because of the reduced positive charge of calixpyridinium from protonated to deprotonated state.[14] Similar experimental phenomenon was observed for SA-M, but only increasing pH from 6 to 7 would lead to a dramatic increase in the optical transmittance of the calixpyridinium−SA-M solution over 700 nm (Figure

DOI: 10.1021/acsomega.8b01554
ACS Omega 2018, 3, 10033−10041

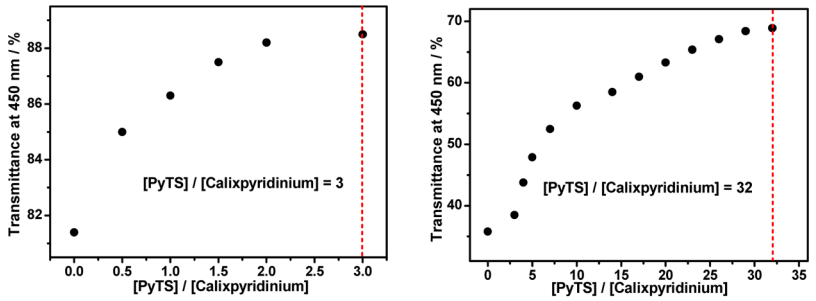

Figure 9. Dependence of the optical transmittance of calixpyridinium−SA-L (a) and calixpyridinium−SA-M (b) assemblies at 450 nm on the concentration ratio of PyTS and calixpyridinium. [Calixpyridinium] = 55 μM, [SA-L] = 50 μg/mL, and [SA-M] = 40 μg/mL.

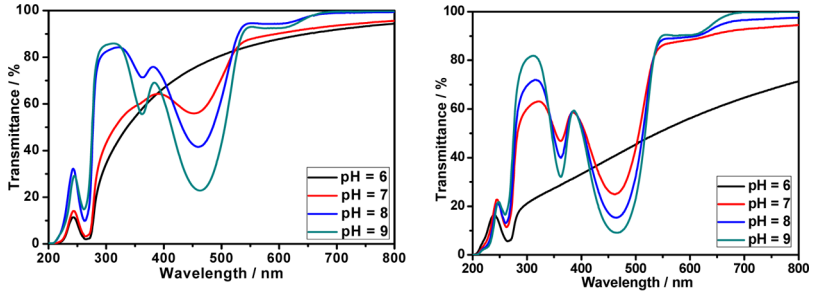

Figure 10. Optical transmittance of the aqueous solutions of the calixpyridinium−SA-L (a) and calixpyridinium−SA-M (b) assemblies at different pH values. [Calixpyridinium] = 55 μM, [SA-L] = 50 μg/mL, and [SA-M] = 40 μg/mL.

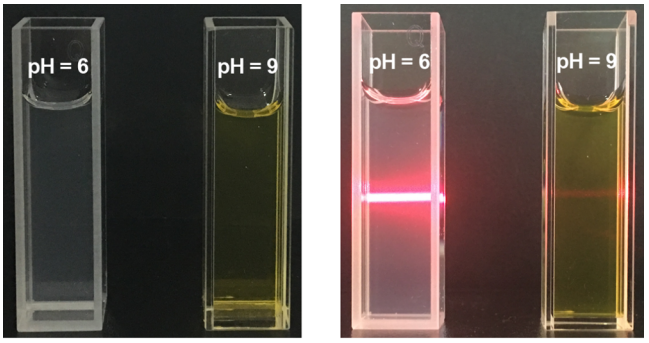

Figure 11. Photos showing the turbidity (a) and Tyndall effect (b) of the calixpyridinium−SA-L solution at pH = 6 and pH = 9 at room temperature in water. [Calixpyridinium] = 55 μM, [SA-L] = 50 μg/mL.

10b). It is reasonable because the electrostatic interaction between calixpyridinium and SA-M is stronger in comparison with calixpyridinium and SA-L, which is more affected by the reduced positive charge of calixpyridinium with increasing the pH value.

On the contrary, as can be seen from Figure 12a, decreasing pH from 6 to 4 would lead to a dramatic decrease in the optical transmittance of the calixpyridinium−SA-L solution, accompanied by a stronger turbidity and the Tyndall effect (Figure S10). One possible explanation for this phenomenon is that the acid radical ions in SA-L would be partially protonated under acidic conditions (Figure S11), which leads to a different supramolecular aggregate formed by calixpyridinium and partially protonated SA-L.[14] However, a completely opposite experimental phenomenon was observed for SA-M. Decreasing pH from 6 to 4 would lead to a little increase in the optical transmittance of the calixpyridinium−SA-M solution (Figure 12b). One possible explanation is that we have proven that

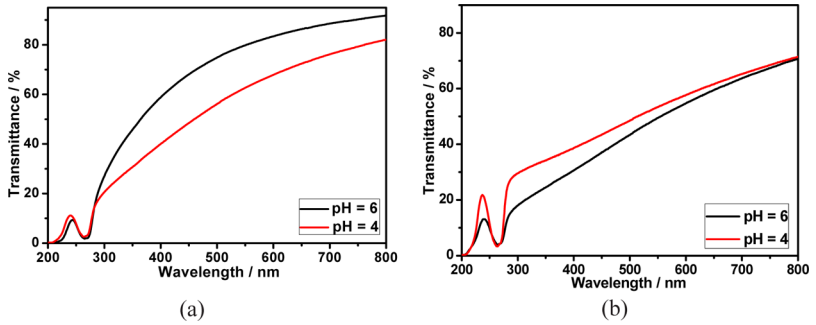

Figure 12. Optical transmittance of the aqueous solutions of the calixpyridinium−SA-L (a) and calixpyridinium−SA-M (b) assemblies at different pH values. [Calixpyridinium] = 55 μM, [SA-L] = 50 μg/mL, and [SA-M] = 40 μg/mL.

DOI: 10.1021/acsomega.8b01554
ACS Omega 2018, 3, 10033−10041

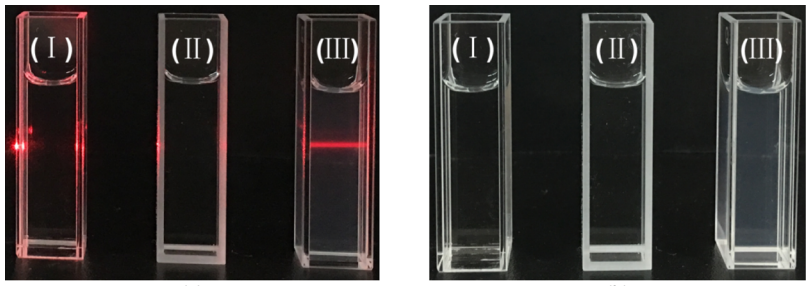

(a) (b)

Figure 13. Photos showing the Tyndall effect (a) and turbidity (b) of free calixpyridinium (I), free SA-L (II), and calixpyridinium−SA-L complex (III) in water, [calixpyridinium] = 55 μM and [SA-L] = 50 μg/mL.

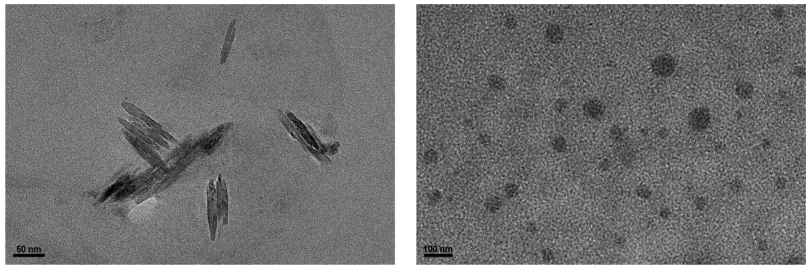

(a) (b)

Figure 14. High-resolution TEM images of the calixpyridinium−SA-L (a) and calixpyridinium−SA-M (b) assemblies. [Calixpyridinium] = 55 μM, [SA-L] = 50 μg/mL, and [SA-M] = 40 μg/mL.

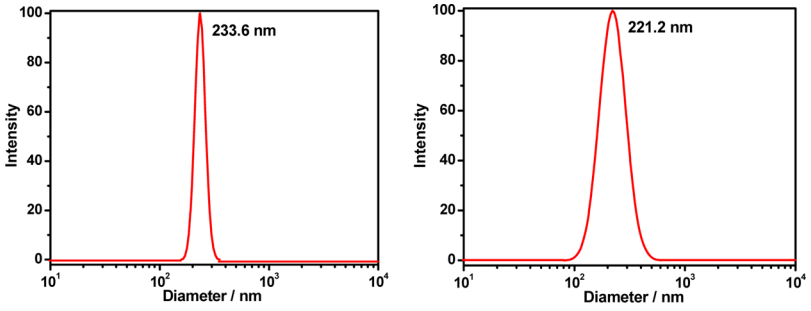

(a) (b)

Figure 15. DLS data of the calixpyridinium−SA-L (a) and calixpyridinium−SA-M (b) assemblies.

calixpyridinium−SA-M supramolecular aggregates are more affected by salt in comparison with calixpyridinium−SA-L supramolecular aggregates, and therefore, generating NaCl with the addition of HCl would lead to a small amount of disassembly of the calixpyridinium−SA-M supramolecular aggregates.

As shown in Figures 13 and S12, a simple mixture of calixpyridinium and SA showed the Tyndall effect and turbidity, revealing that the complexation of calixpyridinium with SA could form abundant nanoparticles. However, free calixpyridinium and SA solutions could not show the similar phenomena, indicating that free calixpyridinium and SA could not self-aggregate under the same conditions. High-resolution transmission electron microscopy (TEM) and dynamic light scattering (DLS) were then employed to characterize the structure and size of the supramolecular aggregates formed by calixpyridinium and SA. The TEM image showed that the morphology of calixpyridinium−SA-L supramolecular aggregates was an incompact lamellar structure (Figure 14a), and DLS examination gave an average diameter of 233.6 nm (Figure 15a), while the morphology of calixpyridinium−SA-M supramolecular aggregates was a compact spherical structure (Figure 14b), and therefore DLS examination gave a little smaller average diameter of 221.2 nm (Figure 15b), which was also in accordance with the abovementioned results that SA-M had a better capability to induce aggregation of calixpyridinium in comparison with SA-L because of the stronger electrostatic interactions of SA-M with calixpyridinium.

3. CONCLUSIONS

In conclusion, we have performed a comparative study on the supramolecular assemblies formed by calixpyridinium and two alginates with different viscosities (SA-L and SA-M). We found that SA-M had a better capability to induce aggregation of calixpyridinium because of the stronger electrostatic interactions of SA-M with calixpyridinium. Therefore, the morphology of calixpyridinium−SA-M supramolecular aggregates was a compact spherical structure, while that of calixpyridinium−SA-L supramolecular aggregates was an incompact lamellar structure. However, for the same reason, in comparison with calixpyridinium−SA-M supramolecular aggregates, calixpyridinium−SA-L supramolecular aggregates

DOI: 10.1021/acsomega.8b01554
ACS Omega 2018, 3, 10033−10041

were much more stable in water not only at room temperature but also at a higher temperature, and even in salt solution. Because SA is an important biomaterial with excellent biocompatibility, it is anticipated that this comparative study is extremely important, not only in further understanding the assembling process of calixpyridinium with polyanions, but also in constructing functional supramolecular biomaterials.

4. EXPERIMENTAL SECTION

4.1. Material Preparation. SA from brown algae of low viscosity (SA-L), SA from brown algae of medium viscosity (SA-M), and PyTS were purchased from Sigma-Aldrich. 1-Methylpyridinium chloride was bought from TCI. These compounds were used directly after purchase. Calixpyridinium was synthesized by a known method.[10] It was characterized by ^{1}H and ^{13}C NMR spectroscopy in D_2O, and X-ray crystallographic analysis using a Bruker AV400 spectrometer and a Bruker APEX-II CCD diffractometer, respectively. Calixpyridinium−SA-L supramolecular assembly was prepared by a simple mixture of calixpyridinium and SA-L in aqueous solution, and it would achieve balance over several minutes. Calixpyridinium−SA-M supramolecular assembly was prepared by a simple mixture of calixpyridinium and SA-M in aqueous solution and it would achieve balance over 2.5 h.

The pH values of the aqueous solutions were adjusted by using HCl and NaOH, and verified by using a Sartorius pp-20 pH meter calibrated with two standard buffer solutions.

4.2. UV/Vis Spectra. A Persee TU-1810 spectrophotometer was used to measure the optical transmittance and UV/vis spectra of the aqueous solution in a quartz cell (light path 10 mm).

4.3. High-Resolution TEM Experiments. A Tecnai G^2 F20 high-resolution transmission electron microscope was used to acquire the high-resolution TEM images operated at an accelerating voltage of 200 keV.

4.4. Centrifuge Tests. Centrifuge tests were performed on a TGL-16G centrifugal machine at 25 °C for 1 min at 3000 rpm.

4.5. DLS and Zeta Potential Measurements. A NanoBrook 173 plus was used to measure the DLS and zeta potential data.

■ ASSOCIATED CONTENT

Supporting Information

The Supporting Information is available free of charge on the ACS Publications website at DOI: 10.1021/acsomega.8b01554.

Detailed experimental procedures, including Figures S1−S12 (PDF)

■ AUTHOR INFORMATION

Corresponding Authors

*E-mail: hxxywk@tjnu.edu.cn (K.W.).
*E-mail: hxxyxsy@tjnu.edu.cn (S.-Y.X.).
*E-mail: hxxyzbl@gmail.com (B.-L.Z.).

ORCID

Kui Wang: 0000-0002-0379-3865
Bo-Lin Zhu: 0000-0002-6846-566X

Notes

The authors declare no competing financial interest.

■ ACKNOWLEDGMENTS

We thank the National Natural Science Foundation of China (21402141, 21302140, and 21572160), the Natural Science Foundation of Tianjin City (18JCQNJC06700), and the Program for Innovative Research Team in University of Tianjin (TD13-5074) for financial support.

■ REFERENCES

(1) (a) Chen, D.; Jiang, M. Strategies for Constructing Polymeric Micelles and Hollow Spheres in Solution via Specific Intermolecular Interactions. *Acc. Chem. Res.* **2005**, *38*, 494−502. (b) Yan, D.; Zhou, Y. F. Supramolecular Self-Assembly of Macroscopic Tubes. *Science* **2004**, *303*, 65−67. (c) Jonkheijm, P.; van der Schoot, P.; Schenning, A. P. H. J.; Meijer, E. W. Probing the Solvent-Assisted Nucleation Pathway in Chemical Self-Assembly. *Science* **2006**, *313*, 80−83.

(2) (a) Wang, C.; Yin, S.; Chen, S.; Xu, H.; Wang, Z.; Zhang, X. Controlled Self-Assembly Manipulated by Charge-Transfer Interactions: From Tubes to Vesicles. *Angew. Chem., Int. Ed.* **2008**, *47*, 9049−9052. (b) Voeltz, G. K.; Prinz, W. A.; Shibata, Y.; Rist, J. M.; Rapoport, T. A. A Class of Membrane Proteins Shaping the Tubular Endoplasmic Reticulum. *Cell* **2006**, *124*, 573−586. (c) Voeltz, G. K.; Rolls, M. M.; Rapoport, T. A. Structural Organization of the Endoplasmic Reticulum. *EMBO Rep.* **2002**, *3*, 944−950. (d) Liu, Y.; Ke, C.-F.; Zhang, H.-Y.; Cui, J.; Ding, F. Complexation-Induced Transition of Nanorod to Network Aggregates: Alternate Porphyrin and Cyclodextrin Arrays. *J. Am. Chem. Soc.* **2008**, *130*, 600−605.

(3) (a) Park, C.; Lee, I. H.; Lee, S.; Song, Y.; Rhue, M.; Kim, C. Cyclodextrin-Covered Organic Nanotubes Derived from Self-assembly of Dendrons and Their Supramolecular Transformation. *Proc. Natl. Acad. Sci. U.S.A.* **2006**, *103*, 1199−1203. (b) Zhang, X.; Chen, Z.; Würthner, F. Morphology Control of Fluorescent Nanoaggregates by Co-Self-Assembly of Wedge- and Dumbbell-Shaped Amphiphilic Perylene Bisimides. *J. Am. Chem. Soc.* **2007**, *129*, 4886−4887.

(4) (a) Wang, Y.; Xu, H.; Zhang, X. Tuning the Amphiphilicity of Building Blocks: Controlled Self-Assembly and Disassembly for Functional Supramolecular Materials. *Adv. Mater.* **2009**, *21*, 2849−2864. (b) Kimizuka, N.; Kawasaki, T.; Kunitake, T. Self-organization of Bilayer Membranes from Amphiphilic Networks of Complementary Hydrogen Bonds. *J. Am. Chem. Soc.* **1993**, *115*, 4387−4388. (c) Kimizuka, N.; Kawasaki, T.; Hirata, K.; Kunitake, T. Supramolecular Membranes. Spontaneous Assembly of Aqueous Bilayer Membrane via Formation of Hydrogen Bonded Pairs of Melamine and Cyanuric Acid Derivatives. *J. Am. Chem. Soc.* **1998**, *120*, 4094−4104. (d) Kim, K.; Jeon, W. S.; Kang, J.-K.; Lee, J. W.; Jon, S. Y.; Kim, T.; Kim, K. A Pseudorotaxane on Gold: Formation of Self-Assembled Monolayers, Reversible Dethreading and Rethreading of the Ring, and Ion-Gating Behavior. *Angew. Chem., Int. Ed.* **2003**, *42*, 2293−2296. (e) Pisula, W.; Kastler, M.; Wasserfallen, D.; Robertson, J. W. F.; Nolde, F.; Kohl, C.; Müllen, K. Pronounced Supramolecular Order in Discotic Donor-Acceptor Mixtures. *Angew. Chem., Int. Ed.* **2006**, *45*, 819−823. (f) Wang, Y.; Ma, N.; Wang, Z.; Zhang, X. Photocontrolled Reversible Supramolecular Assemblies of an Azobenzene-Containing Surfactant with α-Cyclodextrin. *Angew. Chem., Int. Ed.* **2007**, *46*, 2823−2826. (g) Würthner, F. Perylene bisimide dyes as versatile building blocks for functional supramolecular architectures. *Chem. Commun.* **2004**, 1564−1579. (h) Ko, Y. H.; Kim, E.; Hwang, I.; Kim, K. Supramolecular assemblies built with host-stabilized charge-transfer interactions. *Chem. Commun.* **2007**, 1305−1315. (i) Wan, P.; Jiang, Y.; Wang, Y.; Wang, Z.; Zhang, X. Tuning surface wettability through photocontrolled reversible molecular shuttle. *Chem. Commun.* **2008**, 5710−5712. (j) Bize, C.; Garrigues, J.-C.; Blanzat, M.; Rico-Lattes, I.; Bistri, O.; Colasson, B.; Reinaud, O. Spontaneous Formation of Vesicles in a Catanionic Association Involving a Head and Tail Functionalized Amino-calix[6]arene. *Chem. Commun.* **2010**, *46*, 586−588.

(5) (a) Bae, J.; Choi, J.-H.; Yoo, Y.-S.; Oh, N.-K.; Kim, B.-S.; Lee, M. Helical Nanofibers from Aqueous Self-Assembly of an Oligo(p-

DOI: 10.1021/acsomega.8b01554
ACS Omega 2018, 3, 10033−10041

phenylene)-Based Molecular Dumbbell. *J. Am. Chem. Soc.* **2005**, *127*, 9668−9669. (b) Chen, Y.; Zhu, B.; Zhang, F.; Han, Y.; Bo, Z. Hierarchical Supramolecular Self-Assembly of Nanotubes and Layered Sheets. *Angew. Chem., Int. Ed.* **2008**, *47*, 6015−6018. (c) Kunitake, T.; Okahata, Y. A Totally Synthetic Bilayer Membrane. *J. Am. Chem. Soc.* **1977**, *99*, 3860−3861. (d) Stupp, S. I. Supramolecular Materials: Self-Organized Nanostructures. *Science* **1997**, *276*, 384−389. (e) Shimizu, T.; Masuda, M.; Minamikawa, H. Supramolecular Nanotube Architectures Based on Amphiphilic Molecules. *Chem. Rev.* **2005**, *105*, 1401−1444. (f) Zemb, Th.; Dubois, M.; Demé, B.; Gulik-Krzywicki, Th. Self-Assembly of Flat Nanodiscs in Salt-Free Catanionic Surfactant Solutions. *Science* **1999**, *283*, 816−819. (g) Fuhrhop, J. H.; Helfrich, W. Fluid and Solid Fibers Made of Lipid Molecular Bilayers. *Chem. Rev.* **1993**, *93*, 1565−1582. (h) Cates, M. E.; Candau, S. J. Statics and Dynamics of Worm-like Surfactant Micelles. *J. Phys.: Condens. Matter* **1990**, *2*, 6869−6892.

(6) (a) Guo, D.-S.; Chen, K.; Zhang, H.-Q.; Liu, Y. Nano-Supramolecular Assemblies Constructed from Water-Soluble Bis-(calix[5]arenes) with Porphyrins and Their Photoinduced Electron Transfer Properties. *Chem.—Asian J.* **2009**, *4*, 436−445. (b) Perret, F.; Lazar, A. N.; Coleman, A. W. Biochemistry of the Para-Sulfonato-Calix[n]arenes. *Chem. Commun.* **2006**, 2425−2438. (c) Coleman, A. W.; Jebors, S.; Cecillon, S.; Perret, P.; Garin, D.; Marti-Battle, D.; Moulin, M. Toxicity and Biodistribution of Para-Sulfonato-Calix[4]-arene in Mice. *New J. Chem.* **2008**, *32*, 780−782. (d) Wang, K.; Guo, D.-S.; Zhang, H.-Q.; Li, D.; Zheng, X.-L.; Liu, Y. Highly Effective Binding of Viologens byp-Sulfonatocalixarenes for the Treatment of Viologen Poisoning. *J. Med. Chem.* **2009**, *52*, 6402−6412. (e) Uzunova, V. D.; Cullinane, C.; Brix, K.; Nau, W. M.; Day, A. I. Toxicity of Cucurbit[7]uril and Cucurbit[8]uril: An Exploratory in Vitro and in Vivo Study. *Org. Biomol. Chem.* **2010**, *8*, 2037−2042. (f) Stella, V. J.; Rajewski, R. A. Cyclodextrins: Their Future in Drug Formulation and Delivery. *Pharm. Res.* **1997**, *14*, 556−567. (g) Uekama, K.; Hirayama, F.; Irie, T. Cyclodextrin Drug Carrier Systems. *Chem. Rev.* **1998**, *98*, 2045−2076. (h) Zhou, Y.; Li, H.; Yang, Y.-W. Controlled Drug Delivery Systems Based on Calixarenes. *Chin. Chem. Lett.* **2015**, *26*, 825−828. (i) Song, N.; Kakuta, T.; Yamagishi, T.; Yang, Y.-W.; Ogoshi, T. Molecular-Scale Porous Materials Based on Pillar[n]arenes. *Chem* **2018**, *4*. DOI: 10.1016/j.chempr.2018.05.015 (j) Wu, J.-R.; Wang, C.-Y.; Tao, Y.-C.; Wang, Y.; Li, C.; Yang, Y.-W. A Water-Soluble [2]Biphenyl-Extended Pillar[6]arene. *Eur. J. Org. Chem.* **2018**, *2018*, 1321−1325. (k) Wu, J.-R.; Mu, A. U.; Li, B.; Wang, C.-Y.; Fang, L.; Yang, Y.-W. Desymmetrized Leaning Pillar[6]arene. *Angew. Chem., Int. Ed.* **2018**, *57*, 9853−9858.

(7) (a) Kim, K.; Selvapalam, N.; Ko, Y. H.; Park, K. M.; Kim, D.; Kim, J. Functionalized Cucurbiturils and Their Applications. *Chem. Soc. Rev.* **2007**, *36*, 267−279. (b) Liu, Y.; Chen, Y. Cooperative Binding and Multiple Recognition by Bridged Bis(β-cyclodextrin)s with Functional Linkers. *Acc. Chem. Res.* **2006**, *39*, 681−691. (c) Harada, A.; Takashima, Y.; Yamaguchi, H. Cyclodextrin-Based Supramolecular Polymers. *Chem. Soc. Rev.* **2009**, *38*, 875−882. (d) Guo, D.-S.; Liu, Y. Calixarene-Based Supramolecular Polymerization in Solution. *Chem. Soc. Rev.* **2012**, *41*, 5907−5921. (e) Jeon, Y. J.; Bharadwaj, P. K.; Choi, S.; Lee, J. W.; Kim, K. Supramolecular Amphiphiles: Spontaneous Formation of Vesicles Triggered by Formation of a Charge-Transfer Complex in a Host. *Angew. Chem., Int. Ed.* **2002**, *41*, 4474−4476. (f) Zeng, J.; Shi, K.; Zhang, Y.; Sun, X.; Zhang, B. Construction and micellization of a noncovalent double hydrophilic block copolymer. *Chem. Commun.* **2008**, 3753−3755. (g) Yu, G.; Xue, M.; Zhang, Z.; Li, J.; Han, C.; Huang, F. A Water-Soluble Pillar[6]arene: Synthesis, Host-Guest Chemistry, and Its Application in Dispersion of Multiwalled Carbon Nanotubes in Water. *J. Am. Chem. Soc.* **2012**, *134*, 13248−13251. (h) Yu, G.; Zhou, X.; Zhang, Z.; Han, C.; Mao, Z.; Gao, C.; Huang, F. Pillar[6]arene/Paraquat Molecular Recognition in Water: High Binding Strength, pH-Responsiveness, and Application in Controllable Self-Assembly, Controlled Release, and Treatment of Paraquat Poisoning. *J. Am. Chem. Soc.* **2012**, *134*, 19489−19497. (i) Hu, P.; Chen, Y.; Li, J.-J.; Liu, Y. Construction, Enzyme Response, and Substrate Capacity of a Hyaluronan-Cyclodextrin Supramolecular Assembly. *Chem.—Asian J.* **2016**, *11*, 505−511.

(8) (a) Cametti, M.; Rissanen, K. Recognition and sensing of fluoride anion. *Chem. Commun.* **2009**, 2809−2829. (b) Langton, M. J.; Serpell, C. J.; Beer, P. D. Anion Recognition in Water: Recent Advances from a Supramolecular and Macromolecular Perspective. *Angew. Chem., Int. Ed.* **2016**, *55*, 1974−1987.

(9) (a) Atilgan, S.; Akkaya, E. U. A calixpyridinium-pyranine complex as a selective anion sensing assembly via the indicator displacement strategy. *Tetrahedron Lett.* **2004**, *45*, 9269−9271. (b) Wang, T.; Bai, Y.; Ma, L.; Yan, X.-P. Synthesis and Characterization of Indolocarbazole-Quinoxalines with Flat Rigid Structure for Sensing Fluoride and Acetate Anions. *Org. Biomol. Chem.* **2008**, *6*, 1751−1755.

(10) Shinoda, S.; Tadokoro, M.; Tsukube, H.; Shinoda, S.; Arakawa, R. One-step synthesis of a quaternary tetrapyridinium macrocycle as a new specific receptor of tricarboxylate anions. *Chem. Commun.* **1998**, 181−182.

(11) Wang, K.; Cui, J.-H.; Xing, S.-Y.; Dou, H.-X. A Calixpyridinium-Based Supramolecular Tandem Assay for Alkaline Phosphatase and Its Application to ATP Hydrolysis Reaction. *Org. Biomol. Chem.* **2016**, *14*, 2684−2690.

(12) Wang, K.; Cui, J.-H.; Xing, S.-Y.; Ren, X.-W. Selective Recognition of Acidic Amino Acids in Water by Calixpyridinium. *Asian J. Org. Chem.* **2017**, *6*, 1385−1389.

(13) Wang, K.; Cui, J.-H.; Xing, S.-Y.; Ren, X.-W. A hyaluronidase/temperature dual-responsive supramolecular assembly based on the anionic recognition of calixpyridinium. *Chem. Commun.* **2017**, *53*, 7517−7520.

(14) Wang, K.; Ren, X.-W.; Cui, J.-H.; Guo, J.-S.; Xing, S.-Y.; Dou, H.-X.; Wang, M.-M. Multistimuli Responsive Supramolecular Polymeric Nanoparticles Formed by Calixpyridinium and Chondroitin 4-Sulfate. *ChemistrySelect* **2018**, *3*, 2789−2794.

(15) (a) Gorin, P. A. J.; Spencer, J. F. T. Exocellular Alginic Acid from Azotobacter Vinelandii. *Can. J. Chem.* **1966**, *44*, 993−998. (b) Goven, J. R. W.; Fyfe, J. A. M.; Jarman, T. R. Isolation of Alginate-Producing Mutants of Pseudomonas Fluorescens, Pseudomonas Putida and Psuedomonas Mendocina. *J. Gen. Microbiol.* **1981**, *125*, 217−220.

(16) (a) Jiang, Y.-Y.; Zhu, Y.-J.; Li, H.; Zhang, Y.-G.; Shen, Y.-Q.; Sun, T.-W.; Chen, F. Preparation and Enhanced Mechanical Properties of Hybrid Hydrogels Comprising Ultralong Hydroxyapatite Nanowires and Sodium Alginate. *J. Colloid Interface Sci.* **2017**, *497*, 266−275. (b) Stewart, M. B.; Myat, D. T.; Kuiper, M.; Manning, R. J.; Gray, S. R.; Orbell, J. D. A structural basis for the amphiphilic character of alginates - Implications for membrane fouling. *Carbohydr. Polym.* **2017**, *164*, 162−169. (c) Dalheim, M. Ø.; Ulset, A.-S. T.; Jenssen, I. B.; Christensen, B. E. Degradation Kinetics of Peptide-Coupled Alginates Prepared via the Periodate Oxidation Reductive Amination Route. *Carbohydr. Polym.* **2017**, *157*, 1844−1852.

DOI: 10.1021/acsomega.8b01554
ACS Omega 2018, 3, 10033−10041